THE JOURNAL OF PHYSICAL CHEMISTRY Letters

Letter

pubs.acs.org/JPCL

# Design and Characterization of Heteroleptic Ruthenium Complexes Containing Benzimidazole Ligands for Dye-Sensitized Solar Cells: The Effect of Fluorine Substituents on Photovoltaic Performance

Wei-Kai Huang, Hui-Ping Wu, Pi-Lun Lin, Yuan-Pern Lee, and Eric Wei-Guang Diau*

Department of Applied Chemistry and Institute of Molecular Science, National Chiao Tung University, Hsinchu 30010, Taiwan

Supporting Information

**ABSTRACT:** We designed heteroleptic ruthenium complexes (**RD12**–**RD15**) containing fluoro-substituted benzimidazole ligands for dye-sensitized solar cells (DSSCs). These dyes were synthesized according to a typical one-pot procedure with the corresponding ancillary ligands produced in two simple steps; they were prepared into DSSC devices according to the same conditions of fabrication. The eventual devices show a systematic trend of increasing $V_{OC}$ and decreasing $J_{SC}$ with fluorine atoms of increasing number substituted on the ligand. The charge-extraction results show that upward shifts of the $TiO_2$ potential occurred when the fluoro-substituted dyes were sensitized on $TiO_2$ with a systematic trend of shift **N719** > **RD15** (with 5 F) > **RD12** (with 2 F) > **RD5** (no F); the intensity-modulated photovoltage spectra indicate that those fluoro substituents retard charge recombination with the electron lifetimes ($\tau_R$) in the order **RD15** > **RD12** > **RD5** > **N719**, consistent with the variation of $V_{OC}$ for the systems.

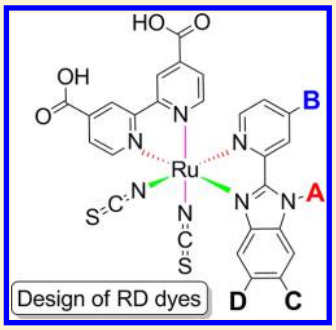


**SECTION:** Energy Conversion and Storage; Energy and Charge Transport

Dye-sensitized solar cells (DSSCs) are promising next-generation photovoltaic devices because of their great advantages of lightweight, low cost, flexibility, and ease of processing.[1,2] As efficient light-harvesting mediators, photosensitizers such as ruthenium complexes,[3,4] zinc porphyrins,[5−8] and metal-free organic dyes[9−11] have been developed and well-investigated. DSSC devices made of homoleptic ruthenium complexes (e.g., **N3** and **N719**) attained a remarkable power conversion efficiency $\eta \approx 11\%$ under one-sun illumination.[12,13] To improve the light-harvesting efficiency via enhancing the absorption coefficient, thiophene-based heteroleptic ruthenium complexes were developed to extend an efficiency of power conversion above 11.5%.[14−16] We previously designed heteroleptic ruthenium complexes containing benzimidazole (BI) ligands for two reasons: first, a BI derivative (TPBI) was used as a hole-blocking layer and electron-transport layer in organic light-emitting diode (OLED) devices exhibiting a small activation voltage because of its great electron mobility;[17] second, BI was used as electrolyte additive in DSSC to shift the conduction band (CB) edge of $TiO_2$ for an enhanced open-circuit voltage ($V_{OC}$) because of its great power to donate electrons.[18] As a result, in that work, the cell performance of the best dye (**RD5**)[19] in the series was found to be comparable to that of a **N719** dye. This promising result has encouraged us to design further a series of heteroleptic ruthenium complexes as highly efficient photosensitizers for DSSC applications.

One strategy to enhance the light-harvesting efficiency of the dye and to improve the long-term stability of the corresponding device is to replace one of the 4,4′-dicarboxylic-2,2′-bipyridine (dcbpy) anchoring ligands in **N3** dye by an ancillary ligand with electron-rich $\pi$-conjugated segments and long alkyl chains.[14−16,20−23] Chart 1 shows the concept for such a molecular design in our approach. The designed heteroleptic ruthenium complex contains only one bidentate dcbpy ligand serving as anchoring group to attach to the surface of $TiO_2$, two monodentate thiocyanate ligands ($SCN^-$) to broaden the absorption spectrum of the complex, and a specific bidentate pyridine-BI ligand comprising four substitutable functional groups labeled **A**, **B**, **C**, and **D** for which a structural modification is readily effected. Compared with other ancillary

**Chart 1. Molecular Design of a Heteroleptic Ruthenium Complex Containing the Benzimidazole Ligand with Possible Substitutions in the A, B, C, and D Positions**

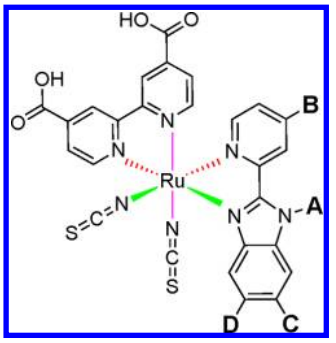


**Received:** May 20, 2012
**Accepted:** June 20, 2012
**Published:** June 20, 2012

  

**Scheme 1. Syntheses of Compound (a), Benzimidazole Ligands L5, L12-L15, and Ruthenium Complexes RD5, RD12−RD15**

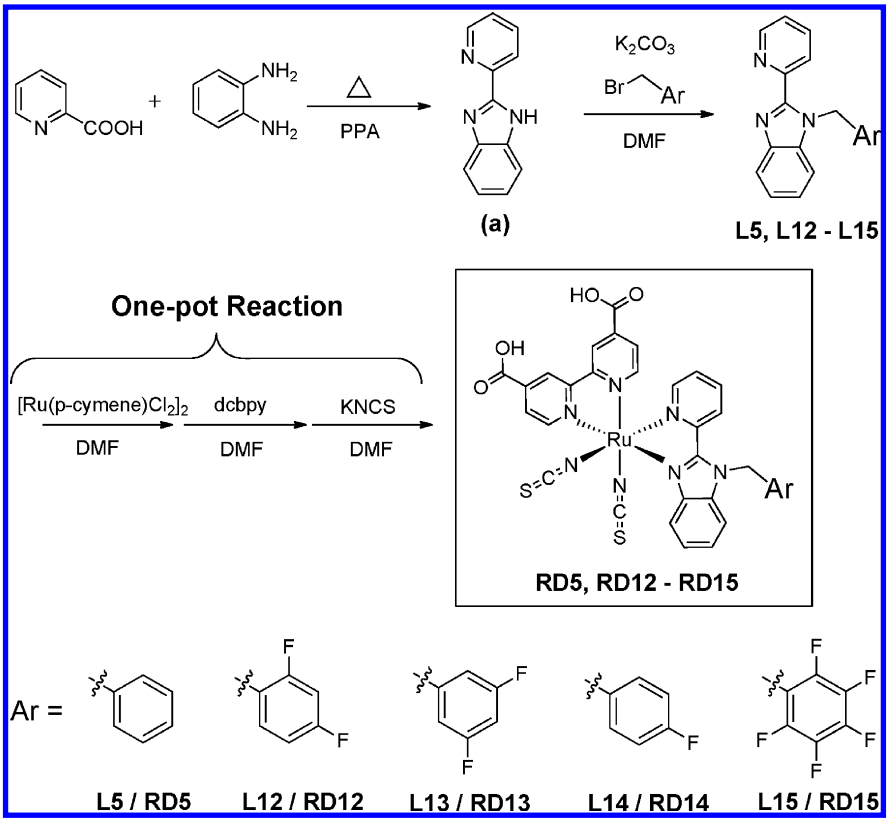


bipyridine-type ligands,[14−16,20−23] the proposed pyridine-BI ligands have more flexibility for a structural design through proper molecular engineering to promote further the device performance. We accordingly undertook systematic investigations for the BI-based Ru complexes with structural modifications in the **A** and **B** positions. In the first part of the present work, only position **A** was modified to give four heteroleptic Ru dyes, **RD12−RD15** (Scheme 1), in which the benzyl-substituted ligand in dye **RD5** was replaced with one fluorobenzyl-substituted ligand with fluorine atoms of varied number attached at various positions of the benzyl ring. It should be mentioned that the motivation for using the fluoro-substituted ligands in **RD12−RD15** came from recent reports of pure organic dyes[24] and other ruthenium complexes.[25,26]

The syntheses of **RD12−RD15** are similar to that of **RD5**.[19] In general, the cyclodehydration and $S_N2$ reactions were used to synthesize the ligands **L12−L15**;[27] a typical one-pot reaction then produced target complexes **RD12−RD15**. The corresponding procedures are summarized in Scheme 1; the details of synthetic procedures and related characterizations are available in the Supporting Information (SI). It is interesting to note that there exist two optical isomers for the ruthenium complexes **RD12−RD15** involving asymmetric ligands. The $^1$H NMR spectra of the **RD12−RD15** dyes are shown in Figures S1a−1d, SI. The NMR spectra are complex because they contain two optical isomers that cannot be separated by using the column chromatography methods such as silica gel, aluminum oxide, or Sephadex LH-20. As a result, the NMR spectra exhibit groups of doublet/multiple peaks in the 7−10 ppm region. Integration of the spectral peaks gives the ratio of the two isomers close to 1:1. Therefore, the average effect of the two inseparable optical isomers should be considered for the results discussed in the following.

Figure 1 presents absorption and emission spectra of **RD5**, **RD12−RD15**, and **N719** in solution; the corresponding

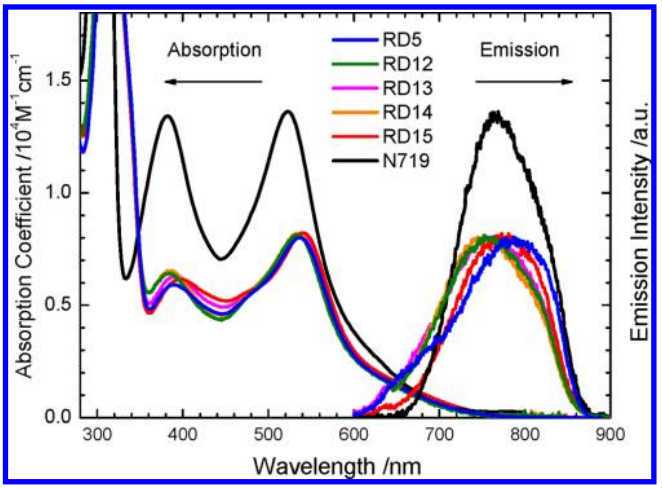


**Figure 1.** Absorption (left) and emission (right) spectra of **RD5**, **RD12−RD15**, and **N719** in DMF ($2 \times 10^{-5}$ M). The positions of the intersection between the two spectra of each species determine the band gap energy $E_{0-0}$ listed in Table S1, SI.

photophysical parameters are summarized in Table S1, SI. The absorption spectra of **RD12−RD15** resemble the spectrum of the **RD5** dye, indicating that the effect of the fluoro substituents on the light-harvesting property is insignificant, but the absorption coefficients of the $^1$MLCT bands of the BI ruthenium complexes are significantly smaller than those of the **N719** dye. The emission spectra of **RD12−RD15** display blue shifts with respect to that of **RD5**; the positions of the


dx.doi.org/10.1021/jz300652z | J. Phys. Chem. Lett. 2012, 3, 1830−1835

intersection with the corresponding absorption spectra determine the band gap energy ($E_{0-0}$) of each species (Table S1, SI).[28]

The electrochemical properties of these Ru dyes were investigated with the cyclic voltammetry (CV) method with a $Fc/Fc^+$ couple as reference; the measured cyclic voltammograms for the oxidation potential ($E_{ox}$) of compounds **RD5**, **RD12**−**RD15**, and **N719** are shown in Figure S2, SI. For each species, the potential level of the HOMO with respect to a normal hydrogen electrode (NHE) was determined from $E_{HOMO} = E_{ox} - E_{Fc/Fc^+} + 0.64$ V, and the potential level of LUMO was determined from $E_{LUMO} = E_{HOMO} - E_{0-0}$; the values of $E_{HOMO}$ and $E_{LUMO}$ are listed in Table S1, SI. Figure 2

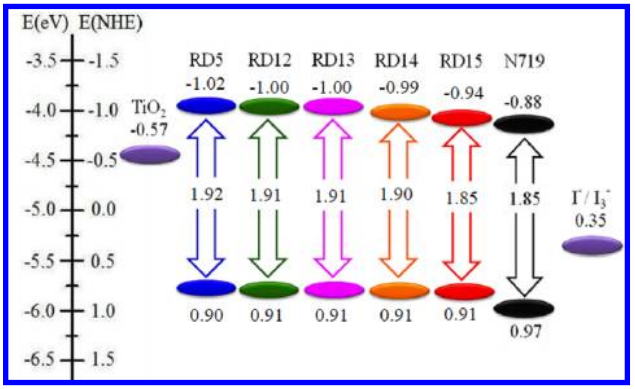


**Figure 2.** Schematic potential levels of **RD5**, **RD12**−**RD15**, and **N719** showing the HOMO and LUMO levels obtained from the electrochemical (Figure S1, SI) and the spectral (Figure 1) measurements.

shows an energy-level diagram of the **RD** dyes for comparison of the HOMO/LUMO levels of each dye with respect to the CB of $TiO_2$ and the potential of the iodide/tri-iodide couple. This diagram shows that the LUMO levels of the **RD** dyes become increasingly stabilized with an increasing number of fluorine atoms, consistent with the electron-withdrawing nature of the fluoro substituents. For all **RD** dyes presented here, both electron injection and dye regeneration are feasible when they serve as photosensitizers for DSSC.

These heteroleptic ruthenium dyes were fabricated into DSSC devices according to the same fabrication with three identical $TiO_2$ films (thickness 12 + 5 $\mu$m); Table S2, SI, summarizes the photovoltaic results of the corresponding devices under standard AM-1.5G illuminations. The photovoltaic performances of these devices show a systematic trend on both $V_{OC}$ and $J_{SC}$ parameters, summarized below. First, the values of $V_{OC}$ increase with fluorine atoms of increasing number in the order **RD15** > **RD13** ∼ **RD12** > **RD14** > **RD5**; the position of the fluoro substituents has no effect on $V_{OC}$ (**RD12** ∼ **RD13**). Second, the values of $J_{SC}$ decrease with fluorine atoms of increasing number in the order **RD5** ∼ **RD14** > **RD12** ∼ **RD13** > **RD15**; the position of the fluoro substituents also has no effect on $J_{SC}$ (**RD12** ∼ **RD13**). As a result, the overall cell performances of these devices exhibit a trend **RD12** ∼ **RD13** ∼ **RD14** > **RD15** ∼ **RD5**. The slightly smaller $J_{SC}$ upon fluorine atoms of increasing number might be due to the lower LUMO levels (Figure 2) and the smaller amount of dye-loading (Table 1) for ligands containing more fluorine atoms. The systematic increase in $V_{OC}$ on increasing the number of fluorine atoms might be due to a potential shift upward upon dye uptake, or retarded charge recombination with the aid of fluoro substituents. To elucidate the effect of fluoro-substituted ligands on the cell performance in detail, we focused our investigations on **RD5** (no fluorine atom), **RD12** (BI ligand with two fluorine atoms), and **RD15** (BI ligand with five fluorine atoms) for comparison with dye **N719**.

The photovoltaic measurements were performed with three identical working electrodes with the thickness of the $TiO_2$ films increasing to 17 + 5 $\mu$m for each dye (**RD5**, **RD12**, **RD15**, and **N719**) under the same experimental conditions. The current−voltage ($J$−$V$) measurements were performed on devices with an active area 4 mm × 4 mm (0.16 $cm^2$) in the absence of the shadow mask. The raw data of each $J$−$V$ measurement are summarized in Table S3, SI; the corresponding averaged photovoltaic parameters are summarized in Table 1. Figure 3a,b shows typical $J$−$V$ curves (working electrode a in supplementary Tables S3, SI) and the corresponding spectra of efficiency of conversion of incident photons to current (IPCE), respectively, for the devices made of each ruthenium dye. Our photovoltaic results demonstrate the same fluoro-substitution effect as those of **RD12**−**RD15** mentioned above (Table S2, SI) with a systematic variation on $V_{OC}$ **N719** > **RD15** > **RD12** > **RD5** and an opposite trend on $J_{SC}$ **RD12** ∼ **RD5** > **RD15** ∼ **N719**. As a result, the overall device performance exhibits a trend **RD12** > **N719** > **RD15** ∼ **RD5**, with the best device (**RD12**) attaining an efficiency 9.5% of power conversion, superior to that of **N719** ($\eta$ = 9.3%) under the same experimental conditions.

An effect of fluorine substituents of the dyes on device performance is reported for pure organic dyes[24] and for ruthenium complexes.[25,26] Although explanations for the observed fluoro-substituted effect were given, no direct evidence was provided. For example, Chen et al.[24] found that a fluorine atom substituted in the ortho position of a donor−acceptor dye performed better than that substituted in the meta position; they speculated that the fluorine atom bearing

**Table 1. Photovoltaic Parameters of DSSC with Photosensitizers RD5, RD12, RD15, and N719 under Simulated AM-1.5G Illumination (Power 100 mW $cm^{-2}$) and Active Area 0.16 $cm^2$ [a]**

| dye | dye loading / nmol $cm^{-2}$ | $J_{SC}$ / mA $cm^{-2}$ | $V_{OC}$ / mV | FF | $\eta$ / % |
|---|---|---|---|---|---|
| **RD5** | 270 | 17.15 ± 0.26 | 732 ± 20 | 0.72 ± 0.02 | 9.07 ± 0.10 |
| **RD12** | 260 | 17.15 ± 0.16 | 756 ± 5 | 0.73 ± 0.01 | 9.49 ± 0.14 |
| **RD15** | 250 | 16.50 ± 0.46 | 764 ± 3 | 0.72 ± 0.03 | 9.08 ± 0.22 |
| **N719** | 170 | 16.57 ± 0.16 | 776 ± 5 | 0.72 ± 0.01 | 9.30 ± 0.12 |

[a]Photovoltaic parameters are averaged values obtained from analysis of the $J$−$V$ curves of three identical working electrodes for each device fabricated and characterized under the same experimental conditions; the raw data of each $J$−$V$ measurement are summarized in Table S3, SI; the uncertainties represent two standard deviations of the measurements.


dx.doi.org/10.1021/jz300652z | J. Phys. Chem. Lett. 2012, 3, 1830−1835

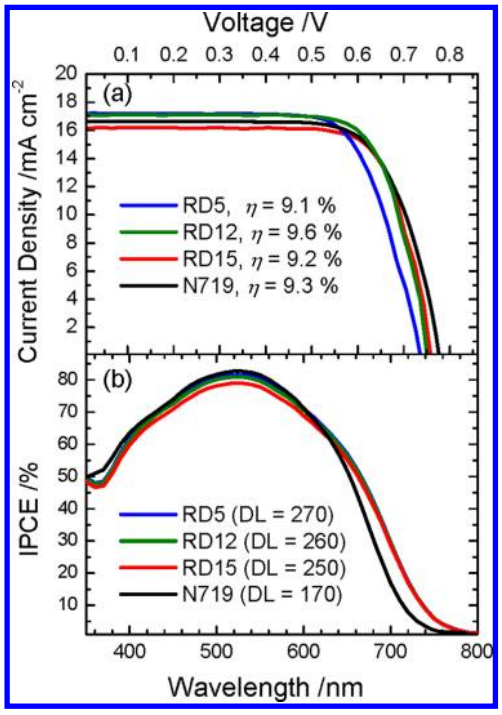


**Figure 3.** Photovoltaic properties: (a) current−voltage characteristics and (b) the corresponding IPCE action spectra of devices made of **RD5**, **RD12**, **RD15**, and **N719** with the same fabricated $TiO_2$ films (17 + 5 $\mu$m) under one-sun AM-1.5G irradiation. The device performances of each dye were measured based on three identical working electrodes (labeled a−c, Table S3, SI), but only the results of device a are displayed in the plots. The amounts of dye loading (DL) shown in panel b are in units nmol cm$^{-2}$.

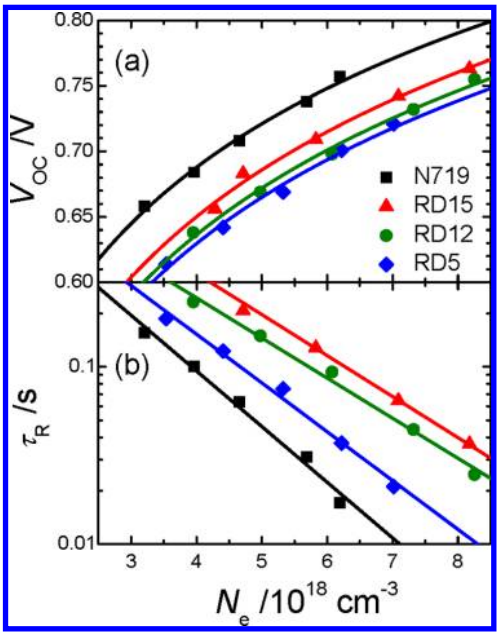


**Figure 4.** (a) Open-circuit voltage ($V_{OC}$) and (b) electron lifetimes ($\tau_R$) as a function of charge densities ($N_e$) for the devices made of **RD5**, **RD12**, **RD15**, and **N719** under five bias light irradiations.

negative partial charge pointed toward the $TiO_2$ surface to increase the potential of $TiO_2$, enabling them to observe $V_{OC}$ greater for the former than for the latter. In our case, we observed a systematic shift upward of the $TiO_2$ potential upon fluoro-substitution, and Chen's interpretation[24] is consistent with our observation. Bessho et al.[25] reported that a thiocyanate-free ruthenium sensitizer with fluoro-substituted cyclometalated ligand performed better than the dye without a fluorine substituent; they attributed such an enhanced cell performance to the adjustment of the Ru(II)/Ru(III) potential induced by the fluorine atoms leading to a rapid dye regeneration. In contrast, Chang et al.[26] found that a ruthenium complex with a BI-based carbene ligand containing no fluorine atoms showed a cell performance better than that of the dye with a fluorobenzyl-substituted ligand. The structure of their fluorine-containing sensitizer resembles that of our dye **RD13** but with carbene coordination instead of nitrogen coordination as in our case. As a result, the fluorine atoms with partial negative charge might be located away from the complex so that the retardation of charge recombination in their case became insignificant.

To account for $V_{OC}$ becoming enhanced upon fluoro substitution, we derived the shift of the CB of $TiO_2$ by measuring the charge densities ($N_e$) for the four devices at each $V_{OC}$ with the charge extraction (CE) method.[29] Figure 4a displays plots of $V_{OC}$ versus $N_e$ for the four systems at five intensities of red light from a LED ($\lambda$ = 610 nm). The CE results indicate that the $TiO_2$ potentials of the devices show a systematic upward shift with the order **N719** > **RD15** > **RD12** > **RD5**, consistent with the variation of their $V_{OC}$. Increasing substitution with fluorine atoms in the phenyl group hence shifts the potential of the CB edge of $TiO_2$ in a more negative direction.

We measured intensity-modulated photovoltage spectra (IMVS) with an ac perturbation (modulation 10%) superimposed on the five cw bias light intensities, the same as in the CE experiments, in the frequency range 0.1−1000 Hz; the frequency of the minimum IMVS response corresponds to the inverse of the electron lifetime ($\tau_R$) of the device under the open-circuit condition. Figure 4b shows plots of $\tau_R$ versus $N_e$ for the four systems at the five light intensities. The results indicate a systematic trend with the electron lifetimes (corresponding to the degree of charge recombination) showing the order **RD15** > **RD12** > **RD5**, which is consistent with the variation of $V_{OC}$ showing the same order for the fluoro-substituted devices. The electron lifetime of the **N719** device is the smallest in the series, indicating that an incorporation of the BI ligands in the **RD** series of dyes effectively retards the charge recombination between the CB electrons on the $TiO_2$ surface and the $I_3^-$ species in the electrolyte. We thus conclude that (1) BI ligands in Ru dyes of this series have the effect of retarding the charge recombination but also leading to a downward shift of the $TiO_2$ potential relative to the **N719** device; (2) substitution with fluorine atoms in the BI ligand produces retarded charge recombination and an upward shift of the $TiO_2$ potential relative to the **RD5** device; (3) increasing substitution of fluorine atoms shifts upward the potential and also decreases the extent of charge recombination; (4) the net effect gives the variation of $V_{OC}$ (**N719** > **RD15** > **RD12** > **RD5**) shown in Figure 2, but the enhanced $V_{OC}$ for **RD15** was too insignificant to compensate for the loss of $J_{SC}$.

In conclusion, heteroleptic ruthenium complexes (**RD12**−**RD15**) containing fluoro-substituted BI ligands were applied to dye-sensitized solar cells. Similar to our approach for dye **RD5**, dyes **RD12**−**RD15** were synthesized according to a typical one-pot procedure; the corresponding heteroleptic ligands were


dx.doi.org/10.1021/jz300652z | J. Phys. Chem. Lett. 2012, 3, 1830−1835

produced in only two simple steps. These dyes were prepared into DSSC devices according to the same conditions of fabrication. The corresponding devices show $V_{OC}$ in the order **RD15** > **RD12** ~ **RD13** > **RD14** > **RD5**; the value of $V_{OC}$ is thus determined by the number of fluorine atoms on the substituted ligands; the trend of $J_{SC}$ for dyes in this series is opposite. To elucidate the effect of the fluorine substituents on cell performance, we measured CE and IMVS at each $V_{OC}$ level. The CE and IMVS results indicate that the increase in $V_{OC}$ upon fluoro-substitution is determined by two factors: an upward shift of potential and a retardation of charge recombination. Increasing substitution with fluorine atoms produces a more negative potential shift, but excess substituted fluorine atoms also result in a decreased $J_{SC}$ because of the lower LUMO level and the smaller amount of dye loading. As a compromise for both $V_{OC}$ and $J_{SC}$, the device made of **RD12** yields the best performance because the potential shift, electron injection, charge recombination, and charge collection are in a balance superior to that of the other systems.

## ■ ASSOCIATED CONTENT

### Ⓢ Supporting Information

Experimental details of syntheses, device fabrication, photovoltaic and impedance investigations, together with supplementary figures and supplementary tables.This material is available free of charge via the Internet at http://pubs.acs.org.

## ■ AUTHOR INFORMATION

### Corresponding Author

*E-mail: diau@mail.nctu.edu.tw. Fax: +886-3-5723764. Tel: +886-3-5131524.

### Notes

The authors declare no competing financial interest.

## ■ ACKNOWLEDGMENTS

We thank Prof. Chien-Chon Chen for providing the Zahner equipment for the CE and IMVS measurements. National Science Council of Taiwan and Ministry of Education of Taiwan, under the ATU program, provided support for this project.

## ■ REFERENCES

(1) Grätzel, M. Recent Advance in Sensitized Mesoscopic Solar Cells. *Acc. Chem. Res.* **2009**, *42*, 1788−1798.

(2) Hagfeldt, A.; Boschloo, G.; Sun, L.; Kloo, L.; Pettersson, H. Dye-Sensitized Solar Cells. *Chem. Rev.* **2010**, *110*, 6595−6663.

(3) Nazeeruddin, M. K.; Kay, A.; Rodicio, I.; Humphry-Baker, R.; Müller, E.; Liska, P.; Vlachopoulos, N.; Grätzel, M. Conversion of Light to Electricity by *cis*-X2bis(2,2′-bipyridyl-4,4′-dicarboxylate)-ruthenium(II) Charge-Transfer Sensitizers (X = Cl-, Br-, I-, CN-, and SCN-) on Nanocrystalline Titanium Dioxide Electrodes. *J. Am. Chem. Soc.* **1993**, *115*, 6382−6390.

(4) Robertson, N. Optimizing Dyes for Dye-Sensitized Solar Cells. *Angew. Chem., Int. Ed.* **2006**, *45*, 2338−2345.

(5) Imahori, H.; Umeyama, T.; Ito, S. Large π-Aromatic Molecules as Potential Sensitizers for Highly Efficient Dye-Sensitized Solar Cells. *Acc. Chem. Res.* **2009**, *42*, 1809−1918.

(6) Martínez-Díaz, M. V.; de la Torre, G.; Torres, T. Lighting Porphyrins and Phthalocyanines for Molecular Photovoltaics. *Chem. Commun.* **2010**, *46*, 7090−7108.

(7) Wang, X.-F.; Tamiaki, H. Cyclic Tetrapyrrole Based Molecules for Dye-Sensitized Solar Cells. *Energy Environ. Sci.* **2010**, *3*, 94−106.

(8) Yella, A.; Lee, H.-W.; Tsao, H. N.; Yi, C.; Chandiran, A. K.; Nazeeruddin, Md. K.; Diau, E. W.-G.; Yeh, C.-Y.; Zakeeruddin, S. M.; Grätzel, M. Porphyrin-Sensitized Solar Cells with Cobalt (II/III)−Based Redox Electrolyte Exceed 12% Efficiency. *Science* **2011**, *334*, 629−634.

(9) Zhang, G.; Bala, H.; Cheng, Y.; Shi, D.; Lv, X.; Yu, Q.; Wang, P. High Efficiency and Stable Dye-Sensitized Solar Cells with an Organic Chromophore Featuring a Binary Pi-Conjugated Spacer. *Chem. Commun.* **2009**, 2198−2100.

(10) Ning, Z.; Tian, H. Triarylamine: A Promising Core Unit for Efficient Photovoltaic Materials. *Chem. Commun.* **2009**, 5483−5495.

(11) Ning, Z.; Fu, Y.; Tian, H. Improvement of Dye-Sensitized Solar Cells: What We Know and What We Need to Know. *Energy Environ. Sci.* **2010**, *3*, 1170−1181.

(12) Nazeeruddin, M. K.; De Angelis, F.; Fantacci, S.; Selloni, A.; Viscardi, G.; Liska, P.; Ito, S.; Takeru, B.; Grätzel, M. Combined Experimental and DFT-TDDFT Computational Study of Photoelectrochemical Cell Ruthenium Sensitizers. *J. Am. Chem. Soc.* **2005**, *127*, 16835−16847.

(13) Wang, Q.; Ito, S.; Grätzel, M.; Fabregat-Santiago, F.; Mora-Seró, I.; Bisquert, J.; Bessho, T.; Imai, H. Characteristics of High Efficiency Dye-Sensitized Solar Cells. *J. Phys. Chem. B* **2006**, *110*, 25210−25221.

(14) Chen, C.-Y.; Wang, M.; Li, J.-Y.; Pootrakulchote, N.; Alibabaei, L.; Ngoc-Ie, C.; Decoppet, J.-D.; Tsai, J.-H.; Grätzel, C.; et al. Highly Efficient Light-Harvesting Ruthenium Sensitizer for Thin-Film Dye-Sensitized Solar Cells. *ACS Nano* **2009**, *3*, 3103−3109.

(15) Cao, Y.; Bai, Y.; Yu, Q.; Cheng, Y.; Liu, S.; Shi, D.; Gao, F.; Wang, P. Dye-Sensitized Solar Cells with a High Absorptivity Ruthenium Sensitizer Featuring a 2-(Hexylthio)thiophene Conjugated Bipyridine. *J. Phys. Chem. C* **2009**, *113*, 6290−6297.

(16) Yu, Q.; Wang, Y.; Yi, Z.; Zu, N.; Zhang, J.; Zhang, M.; Wang, P. High-Efficiency Dye-Sensitized Solar Cells: The Influence of Lithium Ions On Exciton Dissociation, Charge Recombination, and Surface States. *ACS Nano* **2010**, *4*, 6032−6038.

(17) Li, Y. Q.; Fung, M. K.; Xie, Z.; Lee, S.-T.; Hung, L. -S.; Shi, J. An Efficient Pure Blue Organic Light-Emitting Device with Low Driving Voltages. *Adv. Mater.* **2002**, *14*, 1317−1321.

(18) Wang, Q.; Zhang, Z.; Zakeeruddin, S. M.; Grätzel, M. Enhancement of the Performance of Dye-Sensitized Solar Cell by Formation of Shallow Transport Levels under Visible Light Illumination. *J Phys. Chem. C* **2008**, *112*, 7084−7092.

(19) Huang, W.-K.; Cheng, C.-W.; Chang, S.-M.; Lee, Y.-P.; Diau, E. W.-G. Synthesis and Electron-Transfer Properties of Benzimidazole-Functionalized Ruthenium Complexes for Highly Efficient Dye-sensitized Solar Cells. *Chem. Commun.* **2010**, *46*, 8992−8995.

(20) Chen, C.-Y.; Wu, S.-J.; Wu, C.-G.; Chen, J.-G.; Ho, K.-C. Ruthenium Complex with Superhigh Light Harvesting Capacity for Dye-Sensitized Solar Cells. *Angew. Chem, Int. Ed.* **2006**, *45*, 5822−5825.

(21) Gao, F.; Wang, Y.; Zhang, J.; Shi, D.; Wang, M.; Humphry-Baker, R.; Wang, P.; Zakeeruddin, S. M.; Grätzel, M. A New Heteroleptic Ruthenium Sensitizer Enhances the Absorptivity of Mesoporous Titania Film for a High Efficiency Dye-Sensitized Solar Cell. *Chem. Commun.* **2008**, 2635−2637.

(22) Kim, J.-J.; Choi, H.; Kim, C.; Kang, M.-S.; Kang, H. S.; Ko, J. Novel Amphiphilic Ruthenium Sensitizer with Hydrophobic Thiophene or Thieno(3,2-b) Thiophene-Substituted 2,2′-Dipyridylamine Ligands for Effective Nanocrystalline Dye Sensitized Solar Cells. *Chem. Mater.* **2009**, *21*, 5719−5726.

(23) Yen, Y.-S.; Chen, Y.-C.; Hsu, Y.-C.; Chou, H.-H.; Lin, J. T.; Yin, D.-J. Heteroleptic Ruthenium Sensitizers That Contain an Ancillary Bipyridine Ligand Tethered with Hydrocarbon Chains for Efficient Dye-Sensitized Solar Cells. *Chem.—Eur. J.* **2011**, *17*, 6781−6788.

(24) Chen, B.-S.; Chen, D.-Y.; Chen, C.-L.; Hsu, C.-W.; Hsu, H.-C.; Wu, K.-L.; Liu, S.-H.; Chou, P.-T.; Chi, Y. Donor−Acceptor Dyes with Fluorine Substituted Phenylene Spacer for Dye-Sensitized Solar Cells. *J. Mater. Chem.* **2011**, *21*, 1937−1945.

(25) Bessho, T.; Yoneda, E.; Yum, J.-H.; Guglielmi, M.; Tavernelli, I.; Imai, H.; Rothlisberger, U.; Nazeeruddin, M. K.; Grätzel, M. New Paradigm in Molecular Engineering of Sensitizers for Solar Cell Applications. *J. Am. Chem. Soc.* **2009**, *131*, 5930−5934.

(26) Chang, W.-C.; Chen, H.-S.; Li, T.-Y.; Hsu, N.-M.; Tingare, Y. S.; Li, C.-Y.; Liu, Y.-C.; Su, C.; Li, W.-R. Highly Efficient N-Heterocyclic Carbene/Pyridine-Based Ruthenium Sensitizers: Complexes for Dye-Sensitized Solar Cells. *Angew. Chem., Int. Ed.* **2010**, *49*, 8161−8164.
(27) Shavaleev, N. M.; Bell, Z. R.; Easun, T. L.; Rutkaite, R.; Swanson, L.; Ward, M. D. Complexes of Substituted Derivatives of 2-(2-Pyridyl)benzimidazole with Re(I), Ru(II) and Pt(II): Structures, Redox and Luminescence Properties. *Dalton Trans.* **2004**, 3678−3688.
(28) Islam, A.; Sugihara, H.; Arakawa, H. Molecular Design of Ruthenium(II) Polypyridyl Photosensitizers for Efficient Nanocrystalline $TiO_2$ Solar Cells. *J. Photochem. Photobiol., A* **2003**, *158*, 131−138.
(29) Gao, F.; Wang, Y.; Shi, D.; Zhang, J.; Wang, M.; Jing, X.; Humphry-Baker, R.; Wang, P.; Zakeeruddin, S. M.; Grätzel, M. Enhance the Optical Absorptivity of Nanocrystalline $TiO_2$ Film with High Molar Extinction Coefficient Ruthenium Sensitizers for High Performance Dye-Sensitized Solar Cells. *J. Am. Chem. Soc.* **2008**, *130*, 10720−10728.